Acta Crystallographica Section D
**Biological Crystallography**
ISSN 0907-4449

# Improving diffraction by humidity control: a novel device compatible with X-ray beamlines

**Juan Sanchez-Weatherby,[a,b]*‡ Matthew W. Bowler,[c]‡ Julien Huet,[b] Alexandre Gobbo,[b] Franck Felisaz,[b] Bernard Lavault,[b] Raphael Moya,[b] Jan Kadlec,[b] Raimond B. G. Ravelli[d] and Florent Cipriani[b]**

[a]Diamond Light Source Ltd, Diamond House DR1.40, Harwell Science and Innovation Campus, RAL, Chilton, Didcot, Oxfordshire OX11 0DE, England, [b]EMBL Outstation at Grenoble, 6 Rue Jules Horowitz, BP 181, 38042 Grenoble CEDEX 9, France, [c]Structural Biology Group, ESRF, 6 Rue Jules Horowitz, BP 220, 38043 Grenoble CEDEX 9, France, and [d]Section Electron Microscopy, Department of Molecular Cell Biology, Leiden University Medical Center (LUMC), PO Box 9600, 2300 RC Leiden, The Netherlands

‡ These authors contributed equally to this work.

Correspondence e-mail: juan.sanchez-weatherby@diamond.ac.uk



Received 12 June 2009
Accepted 18 September 2009

**PDB References:** $F_1$-ATPase hydration states, 2w6e, r2w6esf; 2w6f, r2w6fsf; 2w6g, r2w6gsf; 2w6h, r2w6hsf; 2w6i, r2w6isf; 2w6j, r2w6jsf.

Dehydration of protein crystals is rarely used, despite being a post-crystallization method that is useful for the improvement of crystal diffraction properties, as it is difficult to reproduce and monitor. A novel device for hydration control of macromolecular crystals in a standard data-collection environment has been developed. The device delivers an air stream of precise relative humidity that can be used to alter the amount of water in macromolecular crystals. The device can be rapidly installed and is fully compatible with most standard synchrotron X-ray beamlines. Samples are mounted in cryoloops and the progress of dehydration can be monitored both optically and by the acquisition of diffraction images. Once the optimal hydration level has been obtained, cryocooling is easy to achieve by hand or by using a sample changer. The device has been thoroughly tested on several ESRF beamlines and is available to users.

## 1. Introduction

Despite the success of macromolecular X-ray crystallography (MX) and continuous advances in the field, the availability of strongly diffracting crystals remains one of the major hurdles for successful structure determination. As projects become more challenging, with more membrane proteins and large multi-component complexes being studied, high solvent contents and weak packing of the molecules are becoming more frequent. The diffraction quality of these crystals is often insufficient to solve the structures.

A number of pre-crystallization techniques exist that are directed at enhancing the diffraction quality of macromolecular crystals; for example, the use of additives, seeding, reengineered constructs, alternative purification methods or cloning of related homologues. These techniques can be costly both in time and resources and assume (often correctly) that once grown, crystals cannot be improved. In contrast, post-crystallization techniques (Heras & Martin, 2005; Newman, 2006) take into consideration the dynamic nature of macromolecular crystals. Proteins usually remain active and are normally capable of short-range and long-range reorganization within the lattice (Morozov & Morozova, 1981, 1983; Morozova & Morozov, 1982; Kachalova *et al.*, 1991). This reorganization is often detrimental to the diffraction qualities of the crystal, but in certain cases can lead to greater internal order, lower solvent content or a change in space group that may result in improved diffraction or a higher quality data set. Further techniques include soaking the crystal with different compounds, chemical cross-linking, crystal annealing and

dehydration, among many others (Abergel, 2004; Juers & Matthews, 2004; Harp *et al.*, 1998; Heras & Martin, 2005; Newman, 2006; Yeh & Hol, 1998). In some cases, a combination of the above has proved to be necessary and successful (Nakamura *et al.*, 2007). There are several ways of implementing these techniques; however, despite having proven to be successful in numerous cases they are rarely used and are generally left for desperate cases. Furthermore, a controlled and systematic study of their effects has not been carried out as in most cases once the diffraction quality is sufficient for structure solution the subject is not pursued further.

Dehydration is a post-crystallization treatment that has been reported to have beneficial effects on diffraction. In some cases this discovery has occurred as a result of a casual observation (cracked capillaries, drops left to dry, badly sealed trays *etc.*; Abergel, 2004; Esnouf *et al.*, 1998). In others it has been the result of a directed experiment to obtain the structure in a dehydrated state (Biswal & Vijayan, 2002; Kaushal *et al.*, 2008; Saraswathi *et al.*, 2002; Sukumar *et al.*, 1999; Madhusudan *et al.*, 1993; Kuo *et al.*, 2003; Bowler *et al.*, 2006*a*; Perutz, 1946; Amunts *et al.*, 2007). Frequently, the effects of dehydration go unnoticed and are attributed to other factors such as crystal handling, new cryoprotectants or intrinsic variability in the crystals.

Several classic methods exist for protein crystal dehydration, including simple air drying, vapour diffusion using salts and soaking with dehydrating compounds (Heras & Martin, 2005; Newman, 2006). The advantage of these methods is that the experiment can be performed with very small humidity steps over long periods of time and that a number of crystals can be modified at the same time. Unfortunately, the outcome of the dehydration is unknown until the experiment is finished

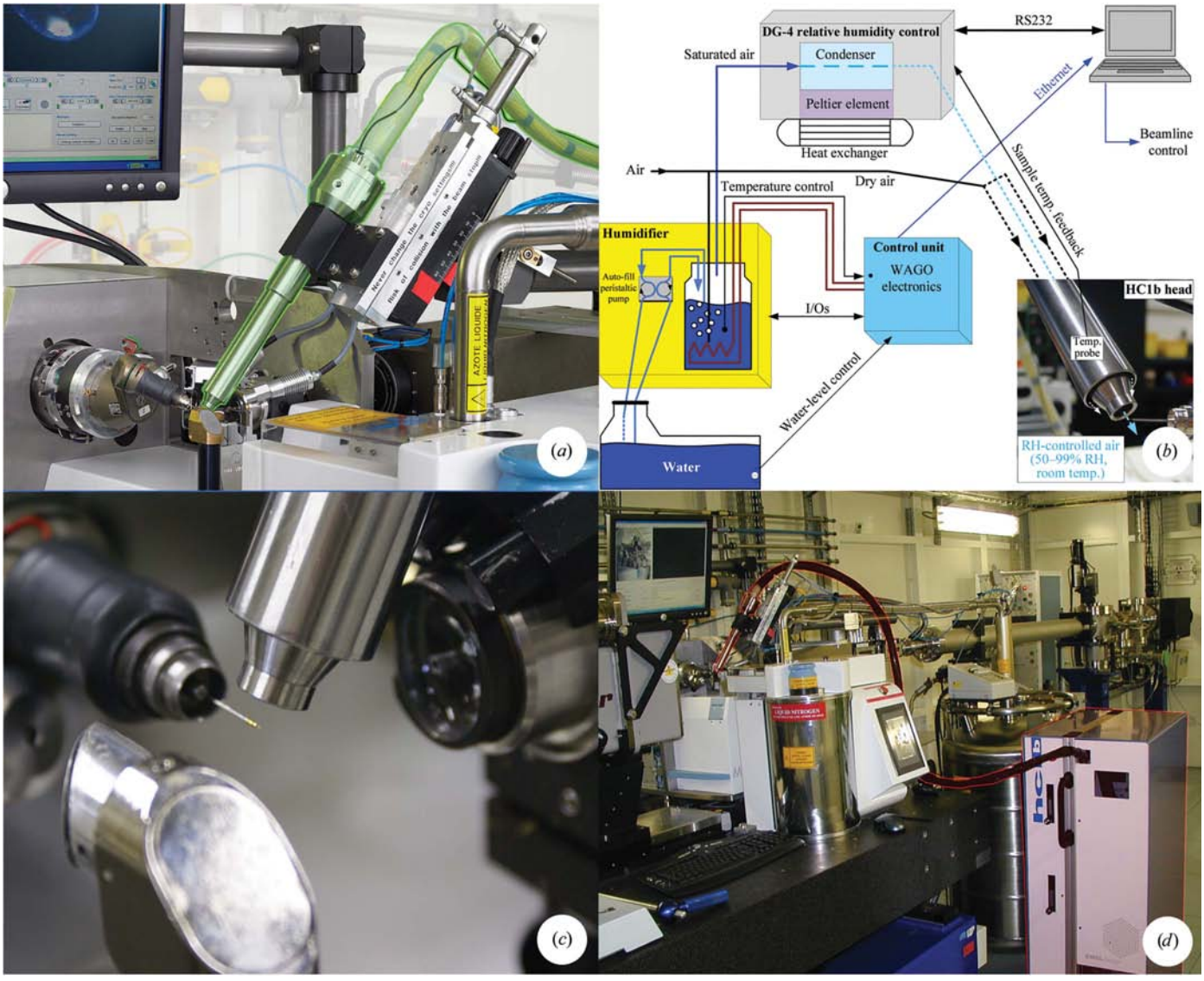


**Figure 1**
The HC1b humidity-control device. (*a*) The HC1b head mounted on a standard ESRF MX beamline. All standard elements are in place, including an open MiniKappa. The red tape shows the vertical position required for the cryo-mount to accommodate the new head. (*b*) Schematic of the HC1b design. (*c*) Enlarged view of the sample environment, showing the spatial constraints that conditioned the design of the nozzle head (note that the beamstop and collimating aperture are not shown). (*d*) The device installed in the experimental hutch of BM14.

and there is no direct way of assessing the progress of the experiment. As this method is crystal- and time-consuming, it is rarely pursued unless there is a prior indication that dehydration could help or there is no alternative.

Most controlled dehydration studies have been carried out using vapour diffusion to regulate the rate of dehydration by using standard salt solutions (Greenspan, 1977). This method has been useful in a number of cases (Heras & Martin, 2005; Newman, 2006), including proteins of medical importance such as HIV reverse transcriptase (Ren *et al.*, 1995; Stammers *et al.*, 1994; Esnouf *et al.*, 1998). The first attempts to create a purpose-built dehydration chamber and thus permit parallel data collection were based on the use of $CaCl_2$ to drive dehydration. Despite being efficient, they were difficult to control and reproduce. Nevertheless, this technique helped to characterize numerous lattice changes in haemoglobin (Huxley & Kendrew, 1953) and a more ergonomic device was subsequently developed (Pickford *et al.*, 1993). Insulin also showed several dehydration transitions (Einstein & Low, 1962) and a modified version of the 1953 dehydration chamber was designed for work with it (Einstein, 1961). The modifications made to the device enabled thermo-regulation above ambient temperature, making it possible to maintain a constant humidity state for several days (Einstein & Low, 1962). This work was the basis for the first gross molecular models of the protein (Einstein *et al.*, 1963; McGavin *et al.*, 1962). The latest addition to vapour-diffusion methodologies has been the MicroRT system. This system, which is based on previous designs using glass capillaries and putty (Skrzypczak-Jankun *et al.*, 1996; Mac Sweeney & D'Arcy, 2003), uses a plastic capillary to surround the sample mounted on a modified copper pin (Kalinin & Thorne, 2005; Kalinin *et al.*, 2005). Dehydration is achieved by changing the content of mother liquor placed at the tip of the capillary. This capillary system is simple and inexpensive but retains the same practical issues as the older methods.

More recently, a free-mounting system (FMS) has been successfully developed and has proven to be very effective (Kiefersauer *et al.*, 1996, 2000). The FMS achieves dehydration *via* a different principle to the device described here, in which two airstreams of 0 and 100% relative humidity (RH) are mixed to achieve the desired RH. A feedback mechanism based on dew-point measurement is used to determine the actual RH, which depends on the temperature of the sample. Variations in humidity are achieved by software control of the streams. The FMS was initially developed as an alternative mounting system. It has been used extensively and a number of successful cases have been documented (Kiefersauer *et al.*, 2000). Despite its success, the FMS requires very careful handling and is difficult to mount and operate within a synchrotron environment.

Better suited to the sample environment is the wet vapour-stream nozzle (Sjögren *et al.*, 2002), which was designed to maintain a crystal at room temperature for spectroscopy studies (Sjögren & Hajdu, 2001*a*,*b*). This nozzle is much better suited for use at a synchrotron as no large modification of the beamline is needed to accommodate it within a standard environment and beamline users do not need to change crystal-mounting techniques. However, control of crystal humidity is difficult with this device.

The lack of a user-friendly apparatus for dehydration experiments sparked an interest in designing a new device that is capable of generating a controlled humid airstream whilst allowing full functionality on most X-ray crystallography beamlines in order for it to be widely and routinely used by the MX community.

## 2. Experimental procedures and results

### 2.1. The main components of the humidity-control device (HC1b)

The simplicity of the device resides in the way it controls the humidity of the airstream. It uses calculation of the dew point to regulate the final RH of the sample in a manner similar to the FMS (Kiefersauer *et al.*, 2000). However, instead of mixing dry and wet airflows to achieve this dew point the device uses a condenser with a Peltier device, which makes it fast to react to temperature fluctuations at the sample position. In this way the air influx is cooled to the calculated temperature, removing the excess water in the condenser, so that the air is at a given RH when it reaches the sample position.

As there is no need to regulate the sample temperature, the airflow at controlled RH can be delivered in a similar fashion to the familiar cryostreams used to cool crystals to 100 K, instead of using a chamber that surrounds the sample (Figs. 1*a* and 1*c*). A safe laminar flow is achieved at flow rates between 3 and 6 l $min^{-1}$ up to a maximum distance from the sample of 1 cm and is protected by a surrounding dry airflow at 10–12 l $min^{-1}$. An internal temperature sensor is used to monitor the humid airstream.

For the prototype, a modified DG-4 Dew Point and Relative Humidity Controller (Sable Systems, Las Vegas, Nevada, USA) was used. Extensive efforts were made to optimize the device parameters in order to achieve the precise regulation required for these experiments.

The DG-4 is supplied with water-saturated air from a bottle containing warm (308 K) water. The dew-point-controlled airstream exits the DG-4 and progresses towards the HC1b nozzle. As the air passes along the connecting tubing, it gradually warms and reaches the tip of the nozzle at a temperature close to ambient. The temperature sensor situated inside the nozzle allows the calculation in real time of the required temperature of the condenser (the dew point) in order to obtain the desired RH at the crystal position (Fig. 1*b*).

In order to permit several days of operation, the water level in the bottle that supplies the saturated air is maintained by a peristaltic pump that refills from a 5 l container. A heating resistor is used to maintain the water temperature at the desired temperature (usually 308 K). A manometer, pressure limiter and pre-filter are installed for safety. A bypass electrovalve isolates the hot-water bottle when the device is switched off. This dries and protects the condenser. The system is controlled by a WAGO PLC (WAGO Kontakttechnik GmbH

& Co. KG) that controls the temperature and automatic filling of the saturated air bottle as well as other safety features of the device.

As there is no inexpensive, fast and precise measurement tool for RH, its measurement is not integrated in the machine (but the dew point is). Nevertheless, to control the long-term stability of the HC1b the following standard saturated salt solutions are used to calibrate the RH: 11.3% LiCl, 32.78% $MgCl_2$, 43.16% $K_2CO_3$, 75.3% NaCl, 84.3% $(NH_4)_2SO_4$ and 97.3% $K_2SO_4$ (Greenspan, 1977). The HC1b is estimated to be accurate to ±0.5% between RH values of 75 and 98%. The stability and speed of regulation depend on the tuning of the condenser temperature regulation. Currently, the calculated RH stability from the (real) condenser temperature and the (real) airstream temperature at the sample position is about ±0.1% r.m.s.d. between RH values of 75% and 99. With this stability, the device is also capable of changing to a new, stable RH at a speed of 30 s per 1% RH.

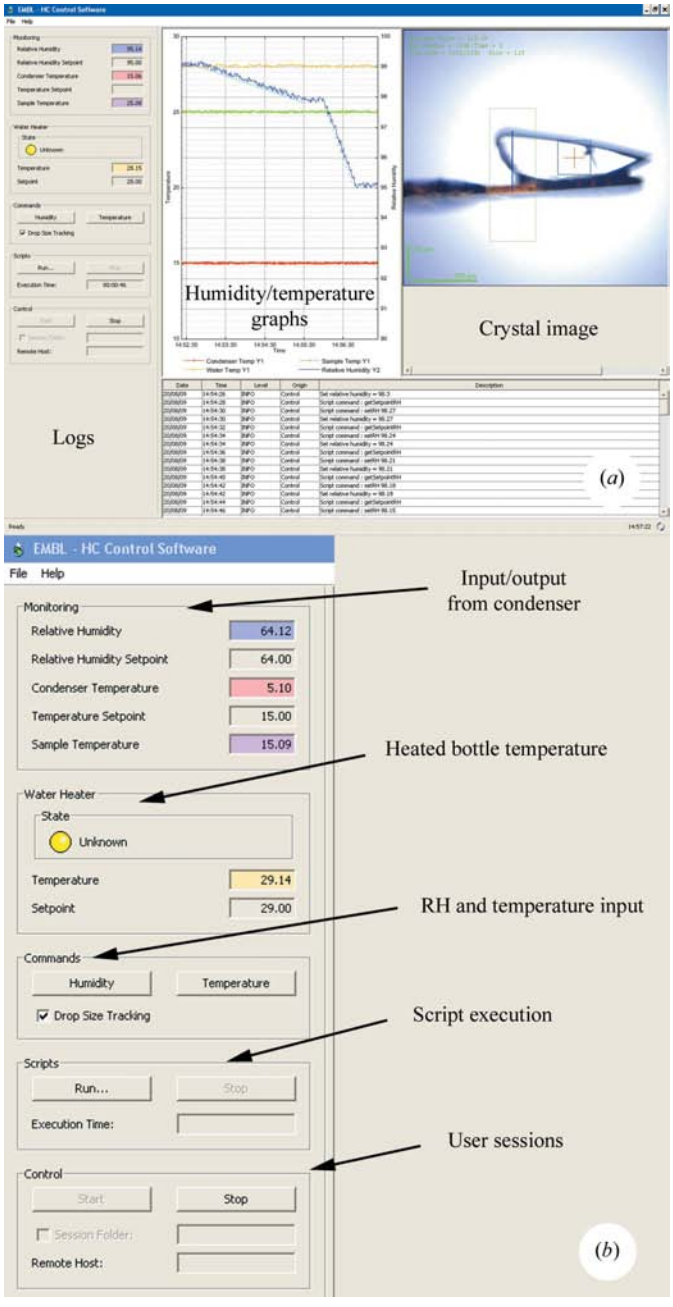


**Figure 2**
The HC1b control software. (*a*) Screen shot of the HC1b software. The control GUI, a step gradient and a crystal being conditioned are shown. (*b*) An enlarged view of the controls tab and the different functions available.

### 2.2. The HC1b on the beamline: the nozzle head

The success of this new equipment at the beamline lies in the design of the air-dispensing nozzle (Figs. 1*a* and 1*b*). The external dimensions are identical to those of a standard Oxford Cryosystems Cryostream (http://www.oxfordcryosystems.co.uk/). As the mounting for the Cryostream already exists, this design allows a rapid change between cryogenic and room-temperature data collection by replacement of the cryonozzle with the HC1b nozzle. The whole process of mounting requires 5–10 min. The operation of all other beamline devices that surround the sample is not affected by the HC1b nozzle (Fig. 1*a* and 1*d*).

Crystals are hand-mounted onto the goniometer. Preference should be given to MicroMesh Mounts (MiTeGen, Ithaca, New York, USA) or Mesh Mounted LithoLoops (Molecular Dimensions, Newmarket, England) as they support the crystals better than nylon loops in dry conditions and allow the removal of mother liquor. Removal of excess mother liquor exposes the crystals completely to the airstream, permitting greater responsiveness to the changes in RH and improved reproducibility. The use of Spine-standard sample holders allows easy crystal cooling/unmounting with compatible sample changers such as the SC3 (Cipriani *et al.*, 2006). In some cases the process of dehydration is sufficient to yield a crystal that will need no penetrative cryoprotectant. However, in some cases finding the right cryocooling conditions requires further handling. This may involve coating the crystals in a suitable cryoprotectant prior to cooling.

In order to achieve better integration at the beamline and full user control, a dual mounting device is being developed to allow both the standard Cryostream and the HC1b head to be mounted permanently on the beamline. With this mounting stand it will be possible to switch quickly between them with no need for technical support.

### 2.3. The HC1b control software

A Java application, scriptable in Python, has been developed to monitor and control humidity changes, display an image of the crystal, collect data and check for diffraction quality with minimum user intervention (Fig. 2). Control of the HC1b is *via* RS232 commands and communication with the host beamline is through an Ethernet connection. The software also displays a graph of the sample temperature ($T_s$), the temperature of the condenser ($T_c$) and the calculated RH. Several standard graphical options are available (rescaling, zooming, cursors *etc.*) and the data can be output as a text file that can be opened in other applications.

**Table 1**
Changes of unit-cell parameters upon dehydration.

Unit-cell parameters are given for the initial and final hydration states of DNA polymerase III, lysozyme and chromatin-modification complex.

| | DNA polymerase III | | Lysozyme ($NO_3$) | | Chromatin-modification complex | |
|---|---|---|---|---|---|---|
| RH (%) | 98 | 88 | >65 | ~60 | 98 | 92 |
| Space group | $P2_12_12_1$ | $P2_12_12_1$ | $P2_12_12_1$ (or $P2_1$) | $P2_1$ | $C222_1$ | $C222_1$ |
| Unit-cell parameters† (Å, °) | $a$ = 83, $b$ = 99, $c$ = 144 | $a$ = 83, $b$ = 94, $c$ = 131 | $a$ = 30, $b$ = 60, $c$ = 60, $\beta$ = 90.5 | $a$ = 30, $b$ = 60, $c$ = 60, $\beta$ = 110 | $a$ = 83, $b$ = 136, $c$ = 128 | $a$ = 78, $b$ = 140, $c$ = 129 |
| Maximum resolution (Å) | 4.0 | 3.0 | 1.5 | 1.2 | 8 | 3.2 |

† $\beta$ is only given where it is other than 90°.

The HC1b control software runs a Java interpreter of Python (Jython) and can be easily scripted, permitting simple programming. Programmed control of the RH can be either stepwise, a gradient or a combination of both. Grabbing of crystal images can also be triggered by the scripts as the software is able to communicate with beamline-control software using the same XML brick used by programs such as *DNA* (Leslie *et al.*, 2002), making it fully compatible with several European synchrotrons. As the software is modular, it is easily adaptable to other beamline environments or home sources.

### 2.4. The dehydration method

**2.4.1. Finding the starting relative humidity**. The HC1b software is also used to find the initial RH that is in equilibrium with the mother liquor. A drop of mother liquor is placed on a standard nylon cryoloop orientated with the plane of the loop perpendicular to the field of view of the inline camera. The image-recognition package *C3D* (Lavault *et al.*, 2006), designed to centre crystals automatically, is used to determine the width and height of the loop and has been modified to recognize the maximum vertical size of a drop of buffer in a loop. This value is plotted in the graph window and updated every second. By monitoring the average maximum height, the RH of the airstream can be modified until it is in equilibrium with the drop. When the drop size is constant, equilibrium has been reached.

**2.4.2. Sample mounting**. Once the equivalent RH for the mother liquor is known, the crystal can be mounted. A mesh loop (Molecular Dimensions or MiTeGen) is centred and then used to mount a crystal. Care needs to be taken as the sample is not held by vitrified mother liquor; it is only held by surface tension to the mesh and may move or fall off the loop. Once the crystal is on the goniometer and centred, the excess liquid is gently wicked away in order to improve water exchange during dehydration.

**2.4.3. Crystal dehydration**. An initial diffraction image is taken to assess the quality of the crystal and to obtain starting unit-cell parameters in order to follow the progress of the experiment. In general, short dehydration steps (0.1–1% in 1–5 min) followed by a short stabilization time (2–5 min) are recommended for initial characterization. X-ray images are taken at different RH points with the minimum exposure time possible in order to minimize radiation damage. Transition points can be established by monitoring diffraction quality, crystal mosaicity, unit-cell parameters, space group and resolution. Once a change is found, the optimal protocol to obtain a positive result must be established. The speed of dehydration, the number of steps and the time of equilibration can all be altered to find the best protocol.

This process requires the sacrifice of some crystals. Dehydration is a slow process and crystals need time to stabilize. Some crystals are very sensitive to radiation and only two to five exposures are possible. Despite the possibility of radiation damage, the use of such a device on a synchrotron beamline allows very precise experiments. It permits detailed understanding of the dehydration transitions involved and quickly provides information as to whether dehydration will be successful.

**2.4.4. Cryocooling**. In order to collect a full data set, optimized crystals need to be cryocooled. Frequently, dehydrated crystals need no cryoprotectant in contrast to nondehydrated crystals. For example, crystals of $F_1$-ATPase require 25% glycerol as cryoprotectant. However, after optimization by dehydration no further cryoprotectant is needed to successfully cryocool the crystals. When crystals are sensitive to cryocooling a cryoprotectant must to be found. The addition of cryoprotectant solutions or oils has been found to be effective in these cases.

### 2.5. Crystallographic methods

Hen egg-white lysozyme (Sigma) was crystallized as described previously (Madhusudan *et al.*, 1993). Briefly, a solution of 100 m*M* $NaNO_3$ and 10 mg ml$^{-1}$ protein was adjusted to a pH of 4.5 with diluted $HNO_3$. Aliquots of 5 ml were incubated at 298 K for several days and once crystals appeared the samples were left at 298 K until data were collected. DNA polmerase III (PolIII) crystals were grown as described previously (Lamers *et al.*, 2006). The protein was kindly provided by Dr Lamers, University of California, Berkeley, USA. Bovine mitochondrial $F_1$-ATPase crystals were kindly donated by Professor Sir John Walker, MRC Mitochondrial Biology Unit, Cambridge. Data were collected on beamlines ID14-1, ID14-2 and the UK MAD beamline BM14 at the European Synchrotron Radiation Facility (ESRF), Grenoble, France.

Data for $F_1$-ATPase hydration states were collected at room temperature (297–301 K). Once a stable state was reached, a strategy to collect the minimum $\varphi$ range (usually 60°) was calculated. The exposure time was kept as low as possible and

**Table 2**
Data-collection and refinement statistics for $F_1$-ATPase hydration-state data sets.

Values in parentheses are for the highest resolution bin.

| $F_1$-ATPase hydration states | State 1 | State 2 | State 3 | State 4A | State 4B | State 5 |
|---|---|---|---|---|---|---|
| PDB code | 2w6e | 2w6f | 2w6g | 2w6h | 2w6i | 2w6j |
| RH (%) | 99.9 | 99.0 | 97.5 | 96.5 | 96.0 | 93.5 |
| Space group | $P2_12_12_1$ | $P2_12_12_1$ | $P2_12_12_1$ | $P2_12_12_1$ | $P2_12_12_1$ | $P2_12_12_1$ |
| Wavelength (Å) | 0.933 | 0.933 | 0.933 | 0.933 | 0.933 | 0.933 |
| Unit-cell parameters (Å) | | | | | | |
| *a* (Å) | 108.5 | 108.0 | 109.4 | 107.7 | 108.9 | 106.9 |
| *b* (Å) | 141.2 | 139.5 | 132.9 | 140.2 | 131.3 | 124.1 |
| *c* (Å) | 285.3 | 280.9 | 275.4 | 268.7 | 267.4 | 264.5 |
| Resolution range (Å) | 60–6.5 | 100–6.0 | 101–6.0 | 62–5.0 | 101–4.0 | 72–3.84 |
| No. of unique reflections | 8205 | 10005 | 22742 | 18314 | 30825 | 32818 |
| Multiplicity | 2.4 (2.2) | 2.4 (2.3) | 2.3 (2.3) | 3.8 (3.8) | 2.5 (2.4) | 2.5 (2.3) |
| Completeness (%) | 91.6 (92.1) | 90.8 (91.7) | 93.7 (96.9) | 99.9 (100) | 93.3 (94.5) | 96.1 (92.8) |
| $R_{\rm merge}$† | 0.23 (0.92) | 0.25 (0.82) | 0.21 (0.69) | 0.20 (0.42) | 0.22 (0.60) | 0.15 (0.26) |
| $\langle I/\sigma(I)\rangle$ | 10.5 (1.1) | 7.9 (1.5) | 7.1 (1.3) | 21.3 (3.4) | 14.3 (1.7) | 11.5 (2.7) |
| Mosaic spread | 0.18 | 0.33 | 0.68 | 0.31 | 0.31 | 0.38 |
| *R* factor‡ (%) | 29 | 34 | 33 | 30 | 30 | 31 |
| Crystal contacts ($\leq$4 Å) | 588 | 1290 | 4254 | 4448 | 6990 | 9354 |

† $R_{\rm merge} = \sum_{hkl}\sum_i |I_i(hkl) - \langle I(hkl)\rangle|/\sum_{hkl}\sum_i I_i(hkl)$, where $\langle I(hkl)\rangle$ is the mean weighted intensity after rejection of outliers. ‡ $R = \sum_{hkl} ||F_{\rm obs}| - |F_{\rm calc}||/\sum_{hkl}|F_{\rm obs}|$, where $F_{\rm obs}$ and $F_{\rm calc}$ are the observed and calculated structure-factor amplitudes.

the oscillation as high as possible in order to limit radiation damage; however, radiation damage was observed after ~30° and this effect limited most data sets to a resolution of 6 Å. It is interesting to note that as the higher ordered states were reached the resolution of the data sets increased to 4 Å. These resolutions were acceptable for determining the changes that occur between symmetry-related molecules during dehydration. Structures were solved by molecular replacement with *MOLREP* (Collaborative Computational Project, Number 4, 1994; Vagin & Teplyakov, 1997) using the native complex (PDB code 1bmf; Abrahams *et al.*, 1994) in which the majority of the $\gamma$-subunit is missing (therefore providing an unbiased model) with all ligands and water molecules removed as a search model. The solution was then subjected to 20 cycles of rigid-body refinement and maps were inspected. The presence of large peaks for the bound nucleotides in the expected subunits was used as a measure of the quality of the solutions. In general, the maps were easily interpretable and secondary-structure elements were straightforward to place into the density from existing structures. *Coot* (Emsley & Cowtan, 2004) was used to build the missing regions in the model into the electron-density maps and to compare the different models. Data-collection and refinement statistics are summarized in Table 2.

### 2.6. The effects of dehydration

The reliability and effectiveness of the device has been tested with several systems (see Tables 1 and 2). Although some of these crystals have previously been described to undergo such transitions, this study demonstrates that the use of such a device at a synchrotron strengthens the fine-tuning of the experiment and enhances the possibility of fully characterizing a given system, thus increasing the chances of finding a suitable dehydration protocol. In addition, the ease and simplicity of its use makes these experiments feasible within a reasonable time.

Among the effects observed are space-group changes, unit-cell shrinkage, mosaic spread changes, spot-profile improvement and increased resolution. Some crystals also undergo an improvement in diffraction resolution and these can be grouped into two different types depending on whether they undergo a single transition or multiple stable transitions.

**2.6.1. *Escherichia coli* DNA PolIII**. The buffer in which *E. coli* DNA polymerase III crystals grow, 15–20% PEG 3350, 0.2–0.35 *M* $NaH_2PO_4$ and 50 m*M* HEPES pH 7.5 (Lamers *et al.*, 2006), is stable at 98% RH. When these crystals are subjected to a descending RH gradient, a decrease in the quality of the diffraction is observed at around 96% RH, such that it is not possible to index the diffraction pattern until the RH reaches 89%, where the diffraction starts to recover. After 5–10 min at 88% RH, diffraction is restored and the resolution limit increases by 1 Å to ~2.8 Å. The crystals undergo a transition; the initial $P2_12_12_1$ unit cell with dimensions of approximately $a$ = 83, $b$ = 99, $c$ = 144 Å is reduced to approximately $a$ = 83, $b$ = 94, $c$ = 131 Å. This corresponds to a 14% total cell-volume reduction and an approximate reduction of the solvent content from 57%(*v*/*v*) to 50%(*v*/*v*).

These crystals have previously been reported to increase their diffraction limits when dehydrated using the FMS (Lamers *et al.*, 2006). Despite the fact that the FMS and the HC1b work in different manners, these crystals undergo the same transition. The changes happen at almost identical RH values and the increase in resolution is comparable. This highlights the robust nature of the method and its reproducibility.

**2.6.2. Hen egg-white lysozyme**. Monoclinic lysozyme is known to undergo a change upon dehydration (Madhusudan *et al.*, 1993; Salunke *et al.*, 1985; Harata & Akiba, 2006). These studies were undertaken using a dry nitrogen stream or sodium chloride solutions and therefore the results were relatively crude. In our hands, these crystals required a starting RH of around 95%. Upon dehydration, no effect was observed until the RH values reached 65%. At this point, the space group changed from orthorhombic $P2_12_12_1$ to monoclinic $P2_1$ in which the $c$ dimension was reduced by half. This was caused by the repositioning of two symmetry-related molecules which become related by the new screw axis in the monoclinic space group. In this case, the diffraction did not appear to significantly increase in resolution; however, it is a

good example of how a similar change could be very useful in achieving collection of a difficult data set. If it were possible to halve a 500–700 Å unit cell, even with the drawback of reduced symmetry, the new space group could greatly facilitate data collection.

**2.6.3. Chromatin-modification complex**. Crystals of a new protein complex involved in chromatin-modification-based transcription regulation (Kadlec *et al.*, in preparation) were tested. These crystals typically diffracted to 8 Å resolution when cryocooled in the presence of standard cryoprotectants. When the crystals were cryoprotected with 25–30% ethylene glycol the diffraction limit could occasionally be increased to 3.5 Å; however, this effect was not easily reproducible and the weak intensity and the smeared shapes of the Bragg peaks were indicative of poor cryoprotection. A complete data set was collected to only 3.6 Å resolution.

The initial RH of the crystallization conditions and the cryoprotectant solution (30% ethylene glycol) were 98% and 80% RH, respectively. This indicated that ethylene glycol was affecting the crystals by dehydrating them. The need for some form of transition explains the variability and difficulty in finding strongly diffracting crystals. It also gives an indication that these crystals are probably relatively resistant to dehydration as they are able to endure the shock of an 18% RH decrease upon cryoprotection.

In their initial state (98% RH) the hydrated crystals showed very little diffraction and images were difficult to index. Upon a rapid dehydration to 96% RH the crystals started to diffract more strongly. This trend continued until 93% RH, where the unit cell observed was $a = 77.9$, $b = 140.3$, $c = 128.8$ Å and some Bragg peaks to a resolution of 3.2 Å were seen. When dehydration was continued, no further improvement was noted until the crystals reached 91% RH, at which point diffraction started to disappear (the macroscopic changes undergone by these crystals during dehydration and rehydration are presented in Supplementary Movie 2[1]).

Crystals were unmounted with the sample changer with no cryoprotection treatment at 93, 92 and 91% RH. Despite the low RH, the resulting diffraction pattern at 100 K showed strong ice rings and a diffraction limit of 3.5 Å. At this low RH other crystals tested are usually cryoprotected. However, in this case extra treatment was required. Two different cryoprotection schemes were tested, adding either a droplet of 30% ethylene glycol or a drop of Perfluoropolyether PFO-X125/03 (Lancaster Synthesis, UK) prior to unmounting the crystal. The oil gave the best results, permitting the collection of a complete data set to 2.8 Å resolution, which was sufficient to build and refine the structure (Kadlec *et al.*, in preparation). The final cryocooled unit cell has dimensions $a = 75.9$, $b = 140.1$, $c = 127.3$ Å, suggesting that most of the improvement arises from contraction of the crystals in the *a* dimension. Once the crystal structure becomes available, further structural analysis should help to understand the detailed interactions by which these crystals improve their internal order.

**2.6.4. Bovine $F_1$-ATPase**. Crystals of bovine $F_1$-ATPase demonstrate a more complex behaviour when subjected to controlled dehydration. These crystals have previously been characterized when dehydrated using the FMS (Bowler *et al.*, 2006*a*,*b*, 2007); however, the ease and simplicity of the new device, coupled with the much greater time resolution that a synchrotron beamline offers, has allowed a much more detailed study of the changes undergone by these crystals upon dehydration. This system can further our understanding of the process of crystal dehydration and may help in defining the general principles involved.

Bovine mitochondrial $F_1$-ATPase crystallizes in the orthorhombic space group $P2_12_12_1$ with unit-cell parameters $a = 108$, $b = 140$, $c = 285$ Å. The crystals are inclined to undergo spontaneous dehydration events in which the *c* unit-cell parameter is reduced to ∼268 Å after an increase in precipitant concentration or crystal handling. This shift occurs rapidly and is energetically favourable as it leads to an increase in the number of crystal contacts without a need to change the existing ones. Further shrinkage of the unit cell has only been observed using controlled dehydration. The ability to collect diffraction images after an exposure of less than a second has allowed us to characterize the transitions undergone by these crystals in great detail. Using the HC1b, it was possible to identify six 'stable' states in the dehydration pathway and to

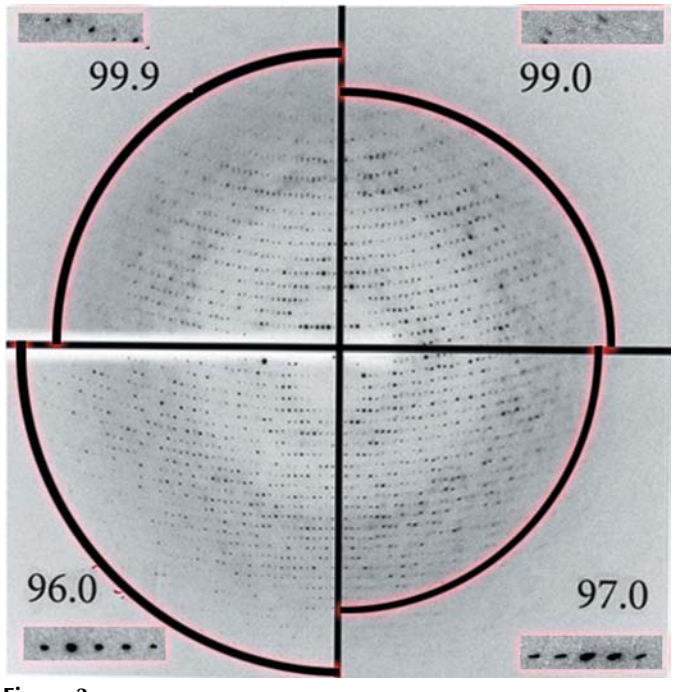


**Figure 3**
Changes in X-ray diffraction of $F_1$-ATPase crystals during dehydration. A crystal was conditioned in four steps (skipping the stable state 2). The four quadrants of the image show the diffraction pattern at each stable dehydration stage (1, 3, 4 and 5). The arc of the circle is at the following resolutions: 3, 3.8, 4 and 2.5 Å. The inserts show a magnified view of the same area on the detector, demonstrating the improvement in Bragg peak profile after dehydration.

[1] Supplementary material has been deposited in the IUCr electronic archive (Reference: GM5010). Services for accessing this material are described at the back of the journal.

collect low-resolution data sets for these states at room temperature to identify changes that occur only during dehydration (see Table 2 for data-collection and refinement statistics). These states were defined by observing diffraction patterns (Fig. 3) with well defined Bragg peaks and a single lattice with distinct unit-cell parameters (if the states were not stable, the Bragg peaks were often split and multiple lattices existed). Together, the structures of these hydration states map the pathway that symmetry-related molecules take as the crystal lattice rearranges (see Supplementary Movie 1 and Fig. 4). At a relative humidity of 99.9% the crystals are in an equilibrium state with the mother liquor (state 1). A minor reduction in the relative humidity to ∼99% leads to state 2, in which the *c* dimension is reduced to 280 Å and there is a doubling in the number of crystal contacts. At this stage the pathway diverges, leading to two possible final states (Fig. 4). A shift to a *c* cell edge of ∼267 Å happens very easily. If this occurs before any decrease in the *b* cell dimension, state 4A is reached (skipping state 3). This state is extremely stable: the foot of the central stalk forms contacts with the N-terminal domain of a $\beta$-subunit from a symmetry-related molecule. Once this state is reached the *b* dimension cannot be reduced, presumably because the lattice contacts formed are too stable (there is a marked improvement in the electron density for these subunits compared with other states). If the crystals proceed to state 3 (with a *c* dimension of 275 Å and, crucially, a *b* dimension of 130 Å) the crystal can then proceed to state 4B (where *c* is reduced to 267 Å) and from there to state 5. State 5 is the most stable form: the *b* and *c* dimensions are further reduced to 124 and 264 Å, respectively, and there is a 25% increase in the number of crystal contacts (Table 1). In this state the crystals exhibit their strongest diffraction properties and the highest data quality. This is mirrored in the statistics for the room-temperature data sets (Table 2), where for this state a complete data set was collected to 3.8 Å. State 5 diffracts around 1 Å better than state 4 and can be readily cryocooled by simply unmounting using the sample changer (Cipriani *et al.*, 2006) without any further treatment. Once cryocooled, these crystals diffracted X-rays to a resolution below 2 Å.

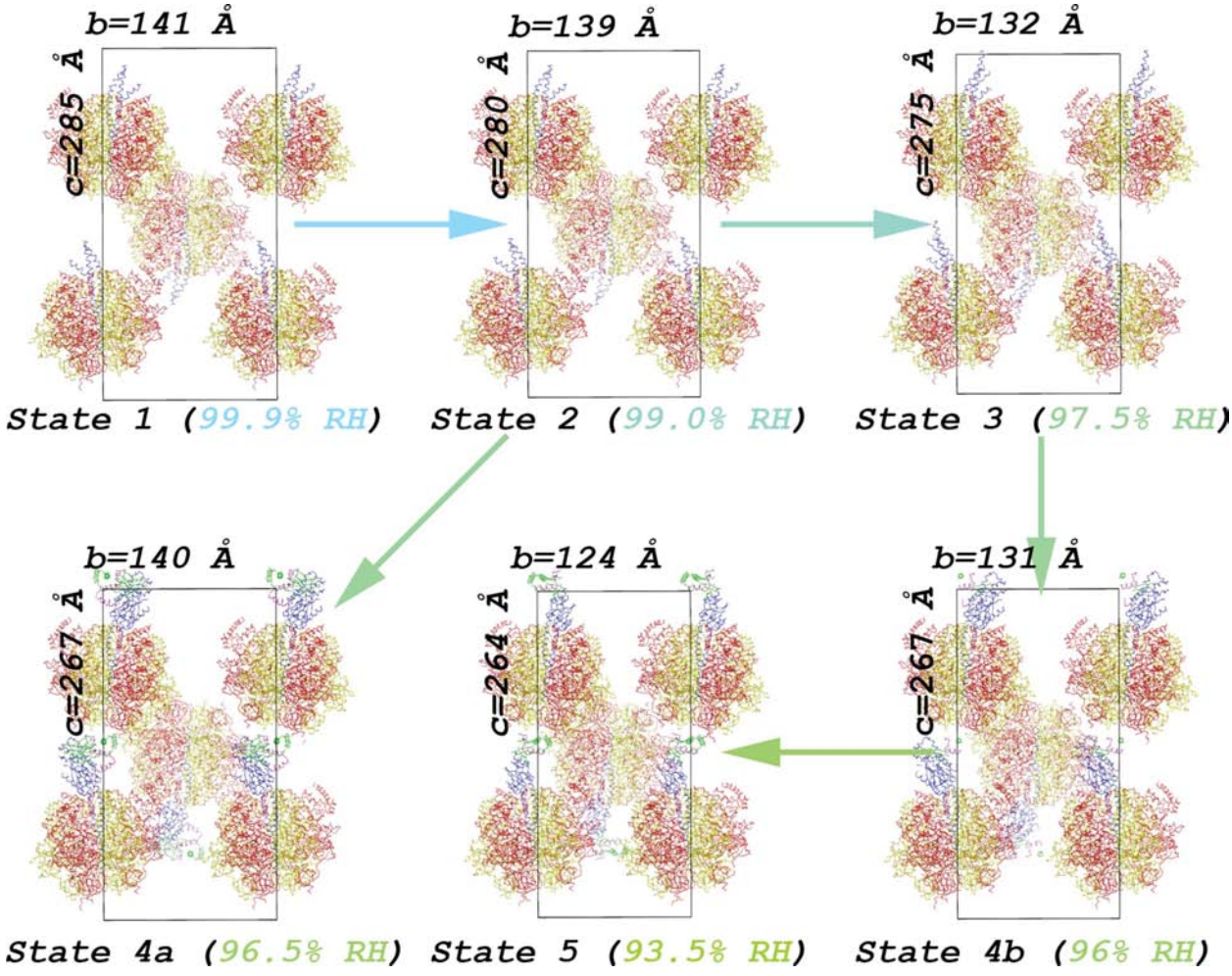


**Figure 4**
The structures of the different transition states of $F_1$-ATPase: crystal packing of $F_1$-ATPase crystals at each dehydration state. The different unit cells are shown viewed along the *a* axis. The asymmetric unit and symmetry-related particles are shown as $C^{\alpha}$ traces coloured by subunit ($\alpha$, red; $\beta$, yellow; $\gamma$, blue; $\delta$, magenta; $\varepsilon$, green). Arrows indicate the different paths that crystals can follow.

It is interesting to note that hydration state 4A seems to be a local energy minimum as the crystals do not readily change to state 5 upon further dehydration. Occasionally, one or two rehydration cycles back to 96% RH can 'loosen' the highly stabilizing crystal contacts, enabling the *b* cell dimension to contract. This suggests that upon the last humidity change the complexes become locked in a particular configuration. This tighter state would only reorganize and thus contract once the pressure on the lattice is released by rehydration. Similar effects have been observed in crystals of carbon monoxide dehydrogenase (CMD) and nitrate reductase (NAP) when dehydrated with the FMS (Kiefersauer *et al.*, 2000). In this case, an initial dehydration step beyond the diffraction optimum is required. Only when crystals are rehydrated does the diffraction improve beyond the original boundary.

This study has enabled a quick crystal-improvement protocol to be set up as the standard tool for conditioning $F_1$-ATPase crystals for high-resolution data collection. A crystal is mounted at 99.9% RH and a diffraction image (0.5 s exposure) is collected. If the diffraction power appears to be reasonable the crystal is subjected to a two-step dehydration gradient. The first step is a fast (2 min) gradient to 96% RH followed by a resting time of 5–10 min. A second slower slope (2 min to 95% RH) is then programmed with a 5–10 min resting time afterwards. At the end of the protocol, the crystal can be unmounted into an empty vial inside the sample changer. Once a number of crystals have been harvested, the Cryostream is remounted and the crystals are tested at 100 K. This method minimizes exposure to X-rays, thus minimizing radiation damage. To avoid using synchrotron time, the conditioning and harvesting process could be performed offline.

## 3. Discussion

From the early stages of protein crystallography, crystal dehydration has been known to affect crystal packing (Perutz, 1946; Huxley & Kendrew, 1953; Berthou *et al.*, 1972; Einstein & Low, 1962). It was a crucial aspect to consider prior to the establishment of cryocooling techniques and considerable effort has been made to understand and control its effects on the crystal lattice (Huxley & Kendrew, 1953; Salunke *et al.*, 1985, Kodandapani *et al.*, 1990; Madhusudan *et al.*, 1993; Esnouf *et al.*, 1998).

Dehydration and other post-crystallization modifications that operate on the crystal lattice are poorly understood. Often, changes are not fully evaluated once structure solution becomes possible. A device such as the HC1b, if well utilized, may prove to be very useful in the understanding of lattice dynamics. From current data, it is already possible to present some general guidelines that may help in the understanding of the dehydration process. Once the device is routinely used by the crystallographic community and more data are available, controlled dehydration should become a standard tool.

Current data suggest that most crystals undergo a transition upon dehydration. Whether this transition has a beneficial or detrimental effect on the diffraction quality depends on the individual packing of the particular sample. For these reasons, the recommended approach to dehydration is to first find the point (or points) of transition in a particular crystal. Once this point has been found, determining the mechanical rearrangements in the transition (including using rehydration) can help in optimizing the experiment. Once the transition is understood, the final stage is to cryoprotect the crystals. Clearly, a suitable number of crystals need to be harvested with the minimum X-ray exposure in order to collect the best possible data set.

Crystal improvement by dehydration is mainly constrained by the possibility of inducing a change to a more ordered state and is not governed by the solvent content of the sample. For this reason it seems that the lower symmetry space groups (triclinic, monoclinic, orthorhombic and tetragonal) have a greater success rate as there are fewer restrictions on the transitions that the symmetry-related molecules can undergo. All crystals in higher symmetry space groups that have been tested showed no improvement in diffraction properties (data not shown).

Furthermore, crystals that have local areas of higher flexibility may also have a good chance of improving. Increasing the number of crystal contacts and decreasing any motion often yields better diffracting crystals. Overall disorder, which is shown by the appearance of split Bragg peaks or a high mosaic spread, can also be corrected by dehydration (Fig. 3). The mechanical forces induced by water loss in the crystal may rearrange local areas of disorder, thus improving spot profiles or mosaic spread. This study documents a number of different effects on crystal behaviour during controlled dehydration that should help in the development of future experiments.

In our hands crystals can undergo single or multiple transitions. These transitions can involve a contraction of some of the unit-cell parameters or a rearrangement of the molecules. The crystal contacts formed (or lost) will determine the quality of the new diffraction pattern. The change in symmetry is achieved by either a loss or gain of symmetry elements, but usually results in a lower number of molecules per asymmetric unit.

The device presented here offers the main advantages of most of the previously available dehydration methods with no major drawbacks. As the device is based on dew-point measurement, it permits easy software control bypassing all the inaccuracies of vapour-diffusion methods. Furthermore, the possibility of using an air nozzle eliminates the handling problems associated with capillaries, copper pins and hydration chambers. Coupled with its use within a synchrotron environment, this simplicity of operation makes the HC1b a quick and easy way to evaluate samples for their response to dehydration. Samples are easy to mount and unmount, including for cryocooling, and they can be easily conditioned and tested. Currently, the HC1b is limited to room-temperature data collection. However, temperature control to 280 K will be possible in the future with a new device (HC2) that is currently being developed.

We would like to thank all the people that have contributed by 'donating' their crystals for testing. Special thanks is given

to M. H. Lamers, J. A. Marquez, M. Montgomery and J. Walker. We would also like to thank the beamline scientists of BM14 and ID14-1 (M. Walsh, H. Belrahali and X. Thibaut) for the allocation of beam time dedicated to testing the new device. Furthermore, we would like to thank the MX Group at the ESRF and the Synchrotron Diffraction Group at the EMBL for their help and support, particularly Dr Sean McSweeney for his comments on the manuscript. Financial support was from the EMBL and the SPINE-2 COMPLEXES, EU FP6 grant reference LSHG-CT-2006-031220.

## References

Abergel, C. (2004). *Acta Cryst.* D**60**, 1413–1416.
Abrahams, J. P., Leslie, A. G. W., Lutter, R. & Walker, J. E. (1994). *Nature (London)*, **370**, 621–628.
Amunts, A., Drory, O. & Nelson, N. (2007). *Nature (London)*, **447**, 58–63.
Berthou, J., Cesbron, F. & Laurent, A. (1972). *J. Mol. Biol.* **71**, 809–813.
Biswal, B. K. & Vijayan, M. (2002). *Acta Cryst.* D**58**, 1155–1161.
Bowler, M. W., Montgomery, M. G., Leslie, A. G. W. & Walker, J. E. (2006*a*). *Acta Cryst.* D**62**, 991–995.
Bowler, M. W., Montgomery, M. G., Leslie, A. G. W. & Walker, J. E. (2006*b*). *Proc. Natl Acad. Sci. USA*, **103**, 8646–8649.
Bowler, M. W., Montgomery, M. G., Leslie, A. G. W. & Walker, J. E. (2007). *J. Biol. Chem.* **282**, 14238–14242.
Cipriani, F. *et al.* (2006). *Acta Cryst.* D**62**, 1251–1259.
Collaborative Computational Project, Number 4 (1994). *Acta Cryst.* D**50**, 760–763.
Einstein, J. R. (1961). *J. Sci. Instrum.* **38**, 449–451.
Einstein, J. R. & Low, B. W. (1962). *Acta Cryst.* **15**, 32–34.
Einstein, J. R., McGavin, A. S. & Low, B. W. (1963). *Proc. Natl Acad. Sci. USA*, **49**, 74–81.
Emsley, P. & Cowtan, K. (2004). *Acta Cryst.* D**60**, 2126–2132.
Esnouf, R. M., Ren, J., Garman, E. F., Somers, D. O'N., Ross, C. K., Jones, E. Y., Stammers, D. K. & Stuart, D. I. (1998). *Acta Cryst.* D**54**, 938–953.
Greenspan, L. (1977). *J. Res. Natl Inst. Stand. Technol.* **81**A, 89–96.
Harata, K. & Akiba, T. (2006). *Acta Cryst.* D**62**, 375–382.
Harp, J. M., Timm, D. E. & Bunick, G. J. (1998). *Acta Cryst.* D**54**, 622–628.
Heras, B. & Martin, J. L. (2005). *Acta Cryst.* D**61**, 1173–1180.
Huxley, H. E. & Kendrew, J. C. (1953). *Acta Cryst.* **6**, 76–80.
Juers, D. H. & Matthews, B. W. (2004). *Acta Cryst.* D**60**, 412–421.
Kachalova, G. S., Morozov, V. N., Morozova, T., Myachin, E. T., Vagin, A. A., Strokopytov, B. V. & Nekrasov, Yu. V. (1991). *FEBS Lett.* **284**, 91–94.
Kalinin, Y., Kmetko, J., Bartnik, A., Stewart, A., Gillilan, R., Lobkovsky, E. & Thorne, R. (2005). *J. Appl. Cryst.* **38**, 333–339.
Kalinin, Y. & Thorne, R. (2005). *Acta Cryst.* D**61**, 1528–1532.
Kaushal, P. S., Sankaranarayanan, R. & Vijayan, M. (2008). *Acta Cryst.* F**64**, 463–469.
Kiefersauer, R., Stetefeld, J., Gomis-Rüth, F. X., Romão, M. J., Lottspeich, F. & Huber, R. (1996). *J. Appl. Cryst.* **29**, 311–317.
Kiefersauer, R., Than, M. E., Dobbek, H., Gremer, L., Melero, M., Strobl, S., Dias, J. M., Soulimane, T. & Huber, R. (2000). *J. Appl. Cryst.* **33**, 1223–1230.
Kodandapani, R., Suresh, C. G. & Vijayan, M. (1990). *J. Biol. Chem.* **265**, 16126–16131.
Kuo, A., Bowler, M. W., Zimmer, J., Antcliff, J. F. & Doyle, D. A. (2003). *J. Struct. Biol.* **141**, 97–102.
Lamers, M. H., Georgescu, R. E., Lee, S. G., O'Donnell, M. & Kuriyan, J. (2006). *Cell*, **126**, 881–892.
Lavault, B., Ravelli, R. B. G. & Cipriani, F. (2006). *Acta Cryst.* D**62**, 1348–1357.
Leslie, A. G. W., Powell, H. R., Winter, G., Svensson, O., Spruce, D., McSweeney, S., Love, D., Kinder, S., Duke, E. & Nave, C. (2002). *Acta Cryst.* D**58**, 1924–1928.
Mac Sweeney, A. & D'Arcy, A. (2003). *J. Appl. Cryst.* **36**, 165–166.
Madhusudan, Kodandapani, R. & Vijayan, M. (1993). *Acta Cryst.* D**49**, 234–245.
McGavin, A. S., Einstein, J. R. & Low, B. W. (1962). *Proc. Natl Acad. Sci. USA*, **48**, 2150–2157.
Morozov, V. N. & Morozova, T. Y. (1981). *Biopolymers*, **20**, 451–467.
Morozov, V. N. & Morozova, T. Y. (1983). *Biofizika*, **28**, 742–747.
Morozova, T. Y. & Morozov, V. N. (1982). *J. Mol. Biol.* **157**, 173–179.
Nakamura, A., Wada, C. & Miki, K. (2007). *Acta Cryst.* F**63**, 346–349.
Newman, J. (2006). *Acta Cryst.* D**62**, 27–31.
Perutz, M. F. (1946). *Trans. Faraday Soc.* **42**, B187–B195.
Pickford, M. G., Garman, E. F., Jones, E. Y. & Stuart, D. I. (1993). *J. Appl. Cryst.* **26**, 465–466.
Ren, J., Esnouf, R., Garman, E., Somers, D., Ross, C., Kirby, I., Keeling, J., Darby, G., Jones, Y., Stuart, D. & Stammers, D. (1995). *Nature Struct. Biol.* **2**, 293–302.
Salunke, D. M., Veerapandian, B., Kodandapani, R. & Vijayan, M. (1985). *Acta Cryst.* B**41**, 431–436.
Saraswathi, N. T., Sankaranarayanan, R. & Vijayan, M. (2002). *Acta Cryst.* D**58**, 1162–1167.
Sjögren, T., Carlsson, G., Larsson, G., Hajdu, A., Andersson, C., Pettersson, H. & Hajdu, J. (2002). *J. Appl. Cryst.* **35**, 113–116.
Sjögren, T. & Hajdu, J. (2001*a*). *J. Biol. Chem.* **276**, 13072–13076.
Sjögren, T. & Hajdu, J. (2001*b*). *J. Biol. Chem.* **276**, 29450–29455.
Skrzypczak-Jankun, E., Bianchet, M. A., Mario Amzel, L. & Funk, M. O. (1996). *Acta Cryst.* D**52**, 959–965.
Stammers, D. K., Somers, D. O'N., Ross, C. K., Kirby, I., Ray, P. H., Wilson, J. E., Norman, M., Ren, J. S., Esnouf, R. M., Garman, E. F., Jones, E. Y. & Stuart, D. I. (1994). *J. Mol. Biol.* **242**, 586–588.
Sukumar, N., Biswal, B. K. & Vijayan, M. (1999). *Acta Cryst.* D**55**, 934–937.
Vagin, A. & Teplyakov, A. (1997). *J. Appl. Cryst.* **30**, 1022–1025.
Yeh, J. I. & Hol, W. G. J. (1998). *Acta Cryst.* D**54**, 479–480.